Supporting Information

Excitation/detection energy controlled anisotropy dynamics

in asymmetrically cyano substituted tri-podal molecules

Kostas Seintis,[a,c] Ioannis Konstantinos Kalis,[a] Milan Klikar,[b] Filip Bureš,[b] Mihalis Fakis[*,a]

[a] Department of Physics, University of Patras, 26504, Greece.

[b] Institute of Organic Chemistry and Technology, Faculty of Chemical Technology, University Pardubice, Studentská 573, Pardubice, Czech Republic.

[c] present address: Department of Physical Chemistry, University of Geneva, 30 Quai Ernest-Ansermet, CH-1211, Geneva, Switzerland.

Synthesis and characterization of 1L and 2L

1L

4-Iodotriphenylamine (175 mg, 0.472 mmol) and ethynylbenzene (72 mg, 0.708 mmol) were dissolved in dry THF (15 ml) and Et$_3$N (5 ml). Argon was bubbled through the solution for 15 min, whereupon [PdCl$_2$(PPh$_3$)$_2$] (17 mg, 0.0236 mmol) and CuI (5 mg, 0.0236 mmol) were added. The reaction mixture was stirred under argon at 25 °C for 48 hours. The solvents were evaporated *in vacuo* and the residue was taken up in aq. NH$_4$Cl (100 ml) and was extracted with of CH$_2$Cl$_2$ (2 × 50 ml). The combined organic extracts were dried (Na$_2$SO$_4$) and the solvents were evaporated *in vacuo*. The crude product was purified by column chromatography (SiO$_2$; pentane/CH$_2$Cl$_2$ 5:1). Oily product was dissolved in hot pentane and solution was placed in the freezer. After precipitation, the solid crystals of **1L** were filtered out and dried. Yield: 135 mg (83 %); white solid. R_f = 0.7 (SiO$_2$; pentane/CH$_2$Cl$_2$ 5:1); mp 93-98 °C. ^{1}H NMR (CDCl$_3$, 500 MHz; 25 °C): δ = 7.50 (d, J = 7.6 Hz, 2H), 7.36 (d, J = 8.5 Hz, 2H), 7.30 − 7.34 (m, 3H), 7.25 − 7.28 (m, 4H), 7.10 (d, J = 7.8 Hz, 4H), 7.05 (t, J = 7.3 Hz, 2H), 7.00 ppm (d, J = 8.5 Hz, 2H). ^{13}C NMR (CDCl$_3$, 125 MHz, 25 °C): δ = 148.1, 147.4, 132.7, 131.7, 129.6, 128.5, 128.1, 125.2, 123.8, 123.7, 122.5, 116.3, 89.8, 88.8 ppm. HR-MALDI-MS (DHB): calcd for C$_{26}$H$_{19}$N (M$^+$) 345.15120, found 345.15143.

2L

4-Iodotriphenylamine (175 mg, 0.472 mmol) and *E*-(2-phenylvinyl)boronic acid pinacol ester (130 mg, 0.566 mmol) were dissolved in the solution of THF/H$_2$O (4:1, 25 ml). Argon was bubbled through the solution for 15 min, whereupon [Pd$_2$(dba)$_3$] (22 mg, 0.0236 mmol), SPhos (10 mg, 0.0236 mmol) and Cs$_2$CO$_3$ (230 mg, 0.708 mmol) were added and the reaction mixture was stirred under argon at 60 °C for 48 hours. The solvents were evaporated *in vacuo* and the residue was taken up in aq. NH$_4$Cl (100 mL) and extracted with of CH$_2$Cl$_2$ (2 × 50 ml). The combined organic extracts were dried (Na$_2$SO$_4$) and the solvents were evaporated *in vacuo*. The crude product was purified by column chromatography (SiO$_2$; pentane/CH$_2$Cl$_2$ 5:1). Oily product was dissolved in hot pentane and solution was placed in the freezer. After precipitation, the solid crystals of **2L** were filtered out and dried. Yield: 120 mg (74 %); yellowish solid. R_f = 0.7 (SiO$_2$; pentane/CH$_2$Cl$_2$ 5:1); mp 151-152 °C. ^{1}H NMR (CDCl$_3$, 500 MHz; 25 °C): δ = 7.48 (d, J = 7.6 Hz, 2H), 7.37 (d, J = 8.3 Hz, 2H), 7.33 (t, J = 7.5 Hz, 2H), 7.21 − 7.27 (m, 5H), 7.10 (d, J = 7.8 Hz, 4H), 6.97 − 7.07 ppm (m, 6H). ^{13}C NMR (CDCl$_3$, 125 MHz, 25 °C): δ = 147.7, 147.5, 137.8, 131.7, 129.5, 128.9, 128.3, 127.6, 127.5, 127.2, 126.5, 124.7, 123.8, 123.2 ppm. HR-MALDI-MS (DHB): calcd for C$_{26}$H$_{21}$N (M$^+$) 347.16685, found 347.16651.

Compound	τ_{rot} (ns)
1a	0.19
1b	0.28
1c	0.32
1d	0.26
2a	0.19
2b	0.25
2c	0.28
2d	0.26

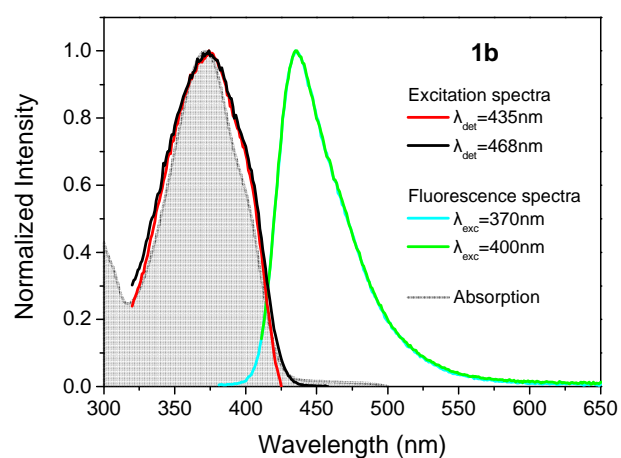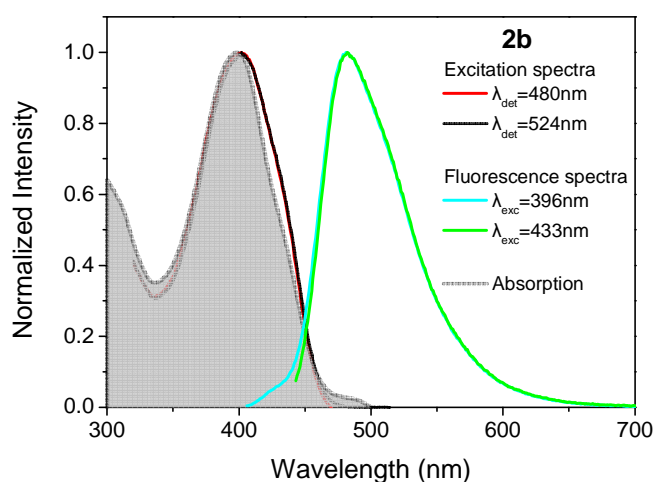Table S1. Long anisotropy lifetimes determined by ns fluorescence measurements for all molecules in TOL.

Figure S1. Fluorescence and excitation spectra for **1b** in TOL for different excitation/detection wavelengths as indicated in the figure. The absorption spectrum is also shown.

Figure S2. Fluorescence and excitation spectra for **2b** in TOL for different excitation/detection wavelengths as indicated in the figure. The absorption spectrum is also shown.
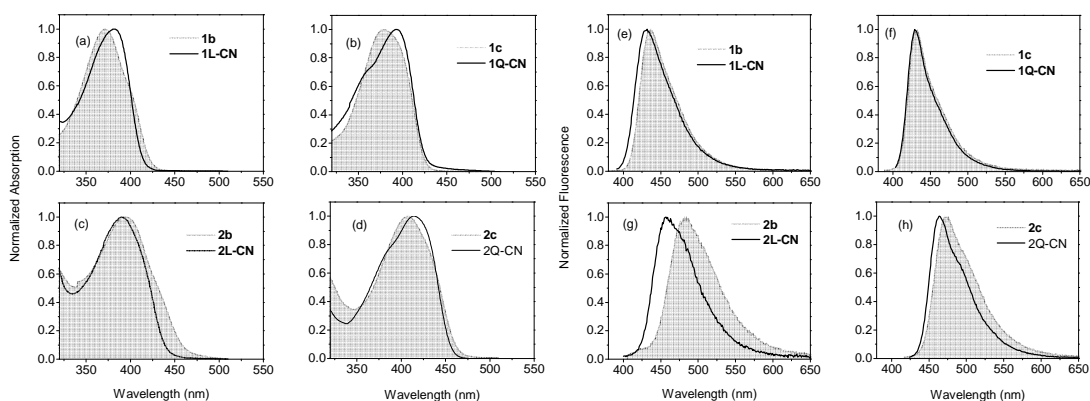
Figure S3. Steady state absorption spectra (a)-(d) and fluorescence spectra (e)-(h) of **1b, 1c** and **2b, 2c** and reference compounds **1L-CN**, **1Q-CN** and **2L-CN** and 2**Q-CN**. All given spectra have been detected in TOL.
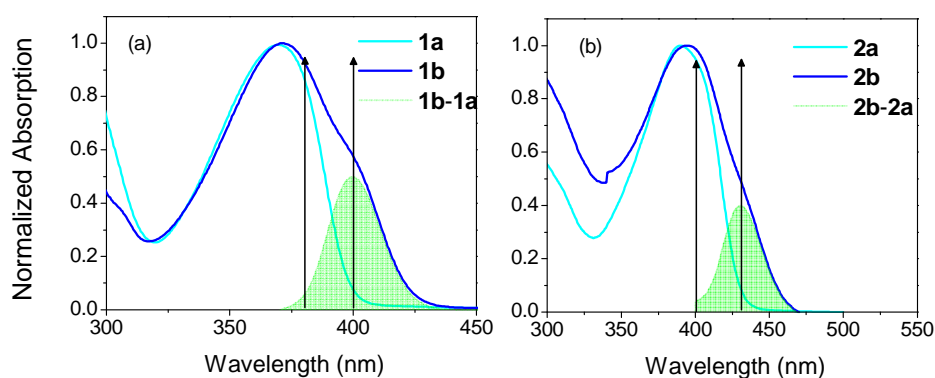

Figure S4. Steady state absorption spectra of (a) **1a** and **1b** and of (b) **2a** and **2b** in TOL. The subtracted spectra are also shown in each figure. The arrows correspond to the excitation wavelengths for the time-resolved fluorescence measurements.
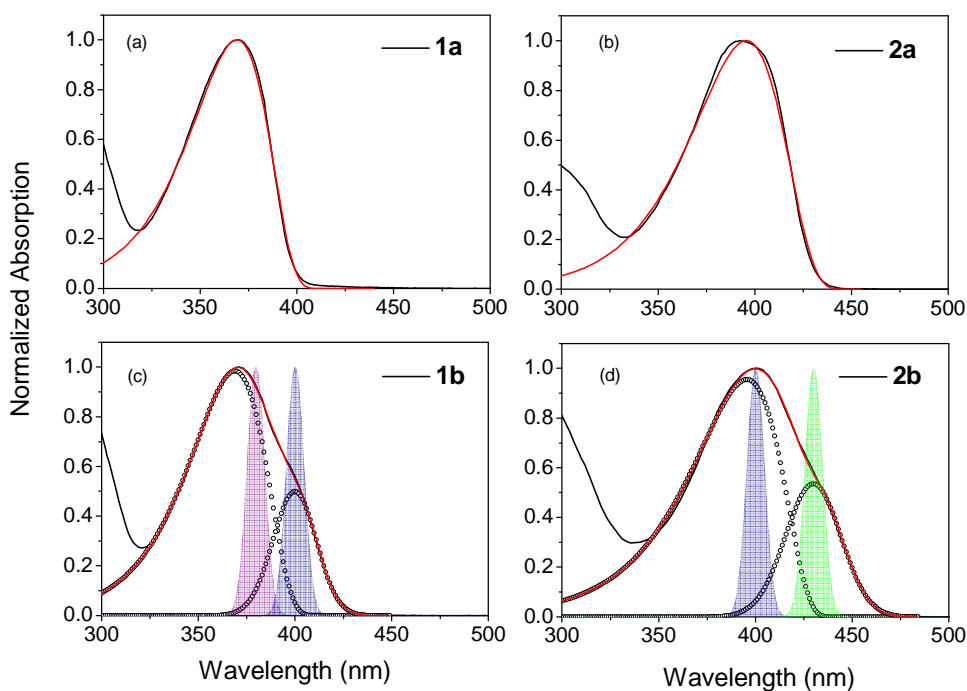
Figure S5. Decomposition of the absorption spectra of **1a**, **1b**, **2a** and **2b** in TOL using a lognormal function or the sum of two lognormal functions depending on the compound. The solid black curves denote the experimental absorption spectra, the red curves are the fits to lognormal functions and the dotted black curves are the decomposed spectra. The magenta, blue and green curves represent the laser spectrum at 380, 400 and 430 nm, respectively. To fit properly the absorption spectra of **1b** and **2b** (above 320 nm), we used the sum of two lognormal functions, one for every state observed in the spectra. The peak position of the first lognormal for **1b(2b)** was kept as a fixed parameter, taken from the fitting of **1a(2a)**. To estimate the peak position of the second lognormal function, we subtracted the spectrum of **1a(2a)** from the spectrum of **1b(2b)** as shown in figure S4 and used the peak of the remaining spectrum as a fixed parameter for the fitting.
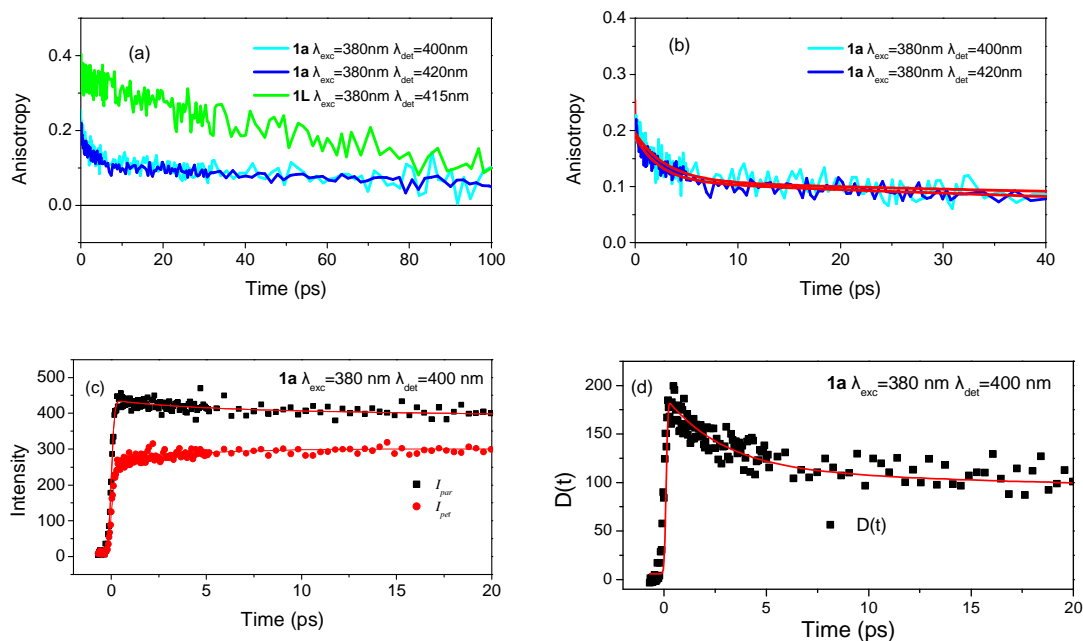
Figure S6. Anisotropy dynamics of compound **1a** in TOL upon excitation at 380 nm and detection at 400 nm and 420 nm as indicated in the figure. The anisotropy dynamics of the reference molecule **1L** is also shown for comparison. Figure (b) shows the anisotropy of **1a** within the 0-40 ps timescale together with fitting curves. Figure (c) shows the decays of $I_{par}(t)$ and $I_{per}(t)$, together with the fitting functions obtained by the equations $I_{par}(t) = (1 + 2r(t))I_{magic}(t)$ and $I_{per}(t) = (1 - r(t))I_{magic}(t)$ convoluted with the IRF. Within this fitting procedure, the lifetime of the magic angle decay has been set constant to 1270 ps derived by ns fluorescence dynamics. Also, the anisotropy has been considered as a bi-exponential function. The lifetime of the long rotational decay has been set constant to 190 ps derived by ns measurements (Table S1). Figure (d) shows the decay of the difference function $D(t) = I_{par}(t) - I_{per}(t)$ and its fitting for **1a** upon excitation at 380 nm and detection at 400 nm.
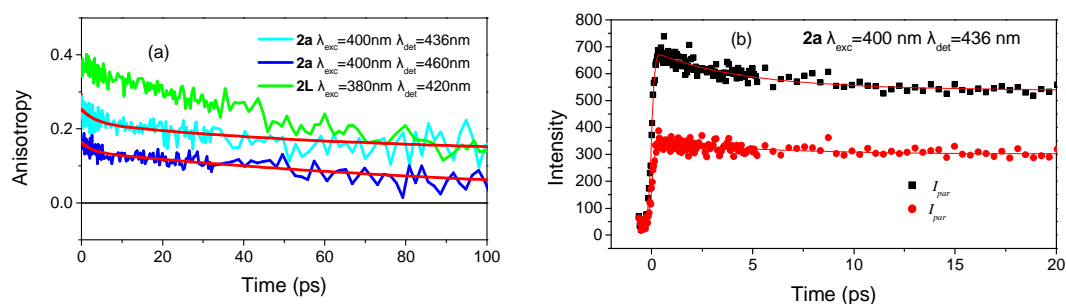

Figure S7. (a) Anisotropy dynamics of compound **2a** in TOL upon excitation at 400 nm and detection at 436 nm and 460 nm as indicated in the figure. The anisotropy dynamics of the reference molecule **2L** is also shown for comparison. (b) The decays of $I_{par}(t)$ and $I_{per}(t)$ for **2a** upon detection at 436 nm, together with the fitting functions obtained by the equations given in the caption of figure S6.
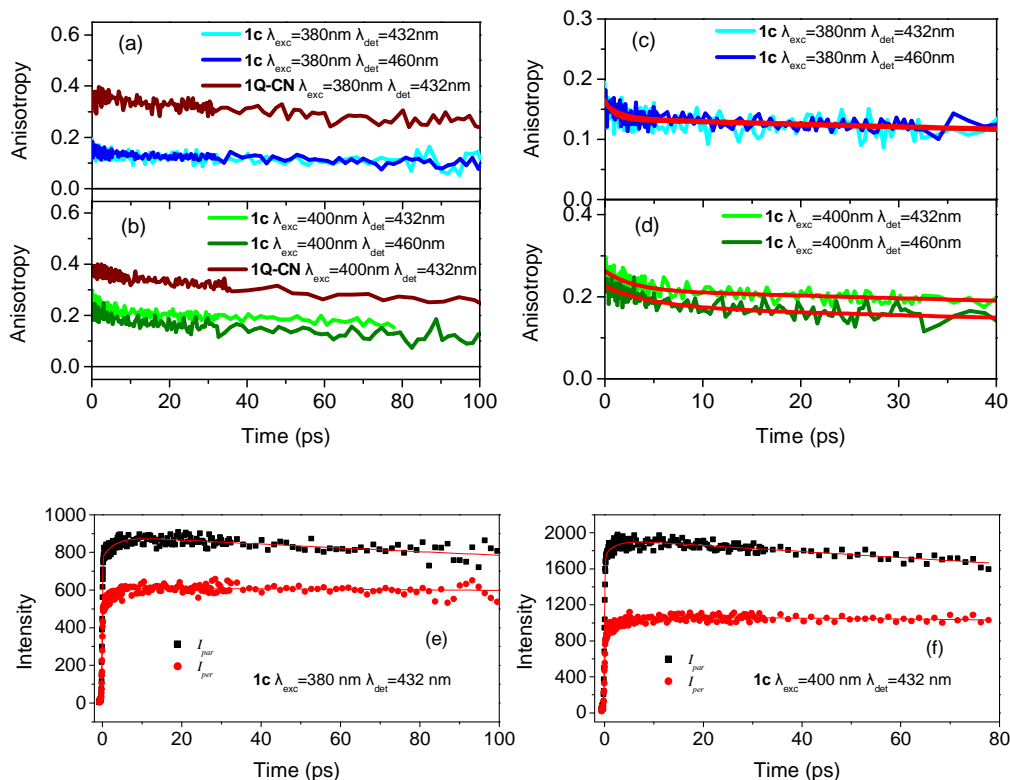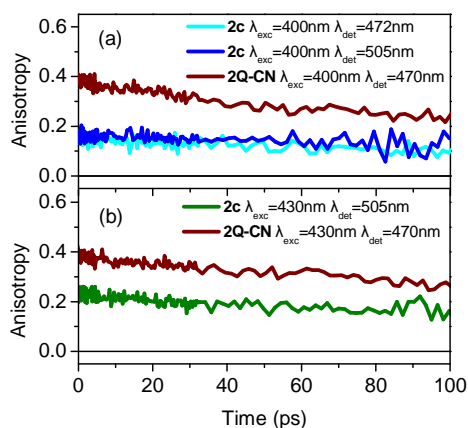
Figure S8. Anisotropy dynamics of compound **1c** in TOL upon excitation at (a) 380 nm and (b) 400 nm and detection at 432 nm and 460 nm as indicated in the figure. The anisotropy dynamics of the reference quadrupolar molecule **1Q-CN** is also shown. Figures (c) and (d) show the anisotropy of **1c** on the 0-40 ps timescale together with fitting function. Figures (e) and (f) provide the decays of $I_{par}(t)$ and $I_{per}(t)$ for **1c** at 432 nm together with fitting functions.

.

Figure S9. Anisotropy dynamics of compound **2c** in TOL upon excitation at (a) 400 nm and (b) 430 nm and detection at 472 nm and 505 nm as indicated in the figure. The anisotropy dynamics of the reference quadrupolar molecule **2Q-CN** is also shown.
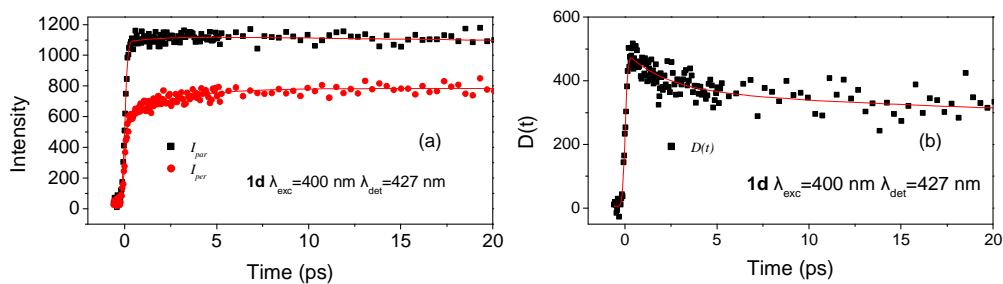
Figure S10. (a) Decays of $I_{par}(t)$ and $I_{per}(t)$ for **1d** in TOL at 427 nm together with fitting functions and (b) the decay of $D(t)$ again with fitting function.
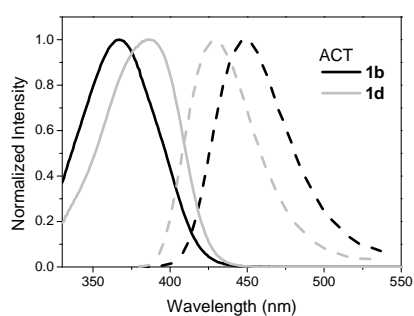

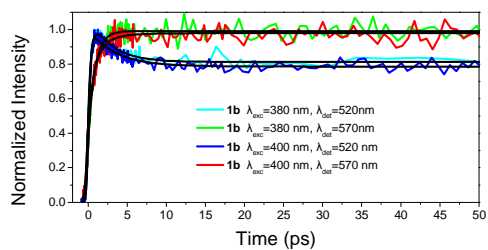Figure S11. Absorption and fluorescence spectra of **1b** and **1d** in ACT.

Figure S12. Fluorescence dynamics within the first 50 ps for **1b** in ACT at different excitation/detection wavelengths.
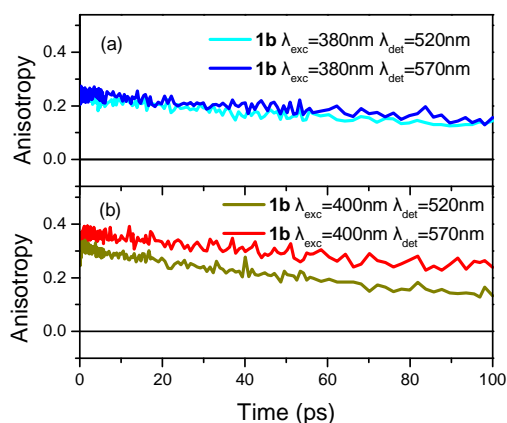
Figure S13. Anisotropy dynamics for compound **1b** in ACT upon excitation at (a) 380 nm and (b) 400 nm and detection at 520 nm and 570 nm as indicated in the figure.
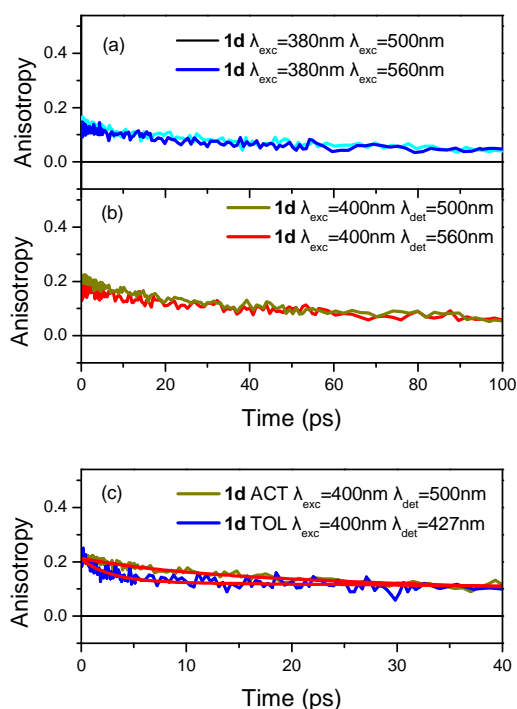

Figure S14. Anisotropy dynamics for compound **1d** in ACT upon excitation at (a) 380 nm and (b) 400 nm and detection at 500 nm and 560 nm as indicated in the figure. Figure (c) shows a comparison of the anisotropy decay of **1d** in ACT and TOL.